Congenital tracheal malformation in cystic fibrosis transmembrane conductance regulator-deficient mice

Elise Bonvin[1,2], Philippe Le Rouzic[1,2], Jean-François Bernaudin[1,3], Charles-Henry Cottart[4], Clarisse Vandebrouck[5,6], Antoine Crié[1], Teresinha Leal[7], Annick Clement[1,2,8] and Monique Bonora[1,2]

[1] *UPMC Université Paris 06, F-75005 Paris, France*
[2] *Inserm, U 719, F-75012 Paris, France*
[3] *EA 3499, F-75020 Paris, France*
[4] *EA 3617, Université René Descartes, Faculté de Pharmacie, F-75005 Paris, France*
[5] *Université de Poitiers, F-86022 Poitiers, France*
[6] *CNRS, UMR 6187, F-86022 Poitiers, France*
[7] *Université Catholique de Louvain, Bruxelles, Belgique*
[8] *AP-HP, Hôpital Trousseau, F-75012, Paris, France*

In cystic fibrosis (CF) patients, the major alteration in pulmonary function is due to peripheral airway obstruction. In the present study, we investigated the possibility that alterations in the extrathoracic airways, particularly in the trachea that expresses high levels of CFTR (CF transmembrane conductance regulator), may contribute to respiratory dysfunction. We performed morphological analyses of the trachea and airway functional studies in adult *Cftr* knockout (*Cftr*$^{-/-}$) and F508del-CFTR mice and their controls. Macroscopic and histological examination of the trachea showed the presence of one to seven disrupted or incomplete cartilage rings in *Cftr*$^{-/-}$ mice (23/25) while only a few *Cftr*$^{+/+}$ mice (6/25) had one abnormal ring. Tracheal defects were mainly localized in the proximal trachea. In 14 *Cftr*$^{-/-}$ mice, frontal disruption of the first three to six rings below the cricoid cartilage were associated with upper tracheal constriction. Similar tracheal abnormalities were detected in adult F508del-CFTR and in newborn *Cftr*$^{-/-}$ and F508del-CFTR mice. Tracheal and ventilatory function analyses showed in *Cftr*$^{-/-}$ mice a decreased contractile response of the proximal trachea and a reduced breathing rate due to an increase in the inspiratory and expiratory times. In F508del-CFTR mice, the expiratory time was longer than in controls. Therefore, these structural and functional abnormalities detected in adult and newborn CF mouse models may represent congenital malformations related to CFTR dysfunction. These results raise important questions concerning the mechanisms governing tracheal development within the context of CFTR protein dysfunction and the implication of such abnormalities in the pathogenesis of airway disease in CF.

(Resubmitted 8 January 2008; accepted after revision 28 April 2008; first published online 1 May 2008)
Corresponding author M. Bonora: Inserm, UMRS 893, Eq 12, Hôpital Saint-Antoine, Bâtiment Kourilsky, 184, rue du Faubourg Saint-Antoine, Paris, 75012 France. Email: bonora@st-antoine.inserm.fr

Cystic fibrosis (CF) is caused by mutations in a gene that encodes a chloride channel, the CF transmembrane conductance regulator (CFTR). Dysfunction of CFTR translates into dehydrated thick secretions causing peripheral airway obstruction with mucus plugging. The main cause of morbidity and mortality in CF is due to a progressive decline in lung function characterized by reduced expiratory flow rates, impairment of respiratory mechanics and abnormal blood gas values (Welsh *et al.* 2001). Moreover, children with CF show impaired ventilatory control associated with a decrease in the ventilatory response to carbon dioxide (CO_2) (Coates *et al.* 1981) and hypoxia (Bureau *et al.* 1981).

Several mouse models harbouring distinct Cftr mutations have been generated (Durie *et al.* 2004). Although CFTR-deficient mice do not develop classical lung disease, some alterations in pulmonary function have been reported in *Cftr*^{tm1Unc} knockout mice homozygous for the S489X mutation (*Cftr*$^{-/-}$) (Kent *et al.* 1996; Cohen *et al.* 2004). Ventilatory measurements carried out in this mouse model, and compared to control mice, showed a lower minute ventilation under room air breathing (Bonora *et al.* 2004; Cottart *et al.* 2007). These modifications of the breathing pattern were not associated with marked histopathological pulmonary changes (Bonora *et al.* 2004; Kent *et al.* 1997). However,

 DOI: 10.1113/jphysiol.2008.150763

disorders of the pulmonary mechanics and breathing pattern could originate from abnormalities in the extrathoracic airways, in particular in the tracheal area which plays a major role in control of breathing (Bartlett, 1989) and contains several sites of CFTR expression. Airway submucosal glands (SMG) are the main site of CFTR expression and mucus production, and thus represent a critical component of the CF lung disease (Engelhardt *et al.* 1992). In mice, SMG have been found to be present and quite abundant in the upper trachea (Borthwick *et al.* 1999; Ianowski *et al.* 2007). In addition, CFTR is expressed in rat tracheal smooth muscle cells and a defect in its function could be directly implicated in abnormal bronchodilatation (Vandebrouck *et al.* 2006).

In the present study, we have investigated the hypothesis that a defect in CFTR may be associated with structural modifications of the trachea that could contribute to an alteration in the tracheal and ventilatory functions. We therefore performed morphological analyses of the trachea and explored tracheal and ventilatory function in adult knockout ($Cftr^{-/-}$) and littermate control ($Cftr^{+/+}$) mice. To determine whether tracheal anomalies are truly related to the CFTR deficit, we also studied the trachea of mice homozygous for the most common clinical mutation (F508del) which is a deletion of a single phenylalanine residue at position 508 that leads to a defective maturation of the CFTR protein (Cheng *et al.* 1990). Finally, by performing morphological analyses of the trachea in newborn animals of the two CF mice models, we explored the possibility that structural alterations in the respiratory system, related to the CFTR deficiency, may result from genetic factors that influence lung development.

Our results show that structural abnormalities of the trachea characterized by defects in cartilaginous rings are present in both newborn and adult $Cftr^{-/-}$ and F508del-CFTR mice. These findings suggest that tracheal abnormalities probably associated with CFTR dysfunction, represent congenital malformations that may contribute to altered tracheal function during adulthood.

Methods

Ethical approval

All experiments were performed in accordance with our Institutional Animal Care and Use Department (Direction Départementale des Services Vétérinaires de Paris, agreement no. B75–1201).

Animals

The study was carried out on two different CF mouse models:

(1) $Cftr^{tm1Unc}$ knockout mice homozygous for the S489X-CFTR mutation (Snouwaert *et al.* 1992), back-crossed into C57BL/6 (three generations) ($Cftr^{-/-}$) and their normal littermates ($Cftr^{+/+}$). Mice were obtained from the CDTA-CNRS (Orléans, France) after weaning at 21–25 days of age. They were housed and bred on corncob pellet bedding and maintained in a specific pathogen-free environment with a 12 h light–dark cycle. Experiments were carried out on 4-month-old male and female mice.

(2) $Cftr^{tm1Eur}$ mice homozygous for the F508del mutation of CFTR in the 129/FVB (van Doorninck *et al.* 1995) outbreed background F508del-CFTR ($\Delta F/\Delta F$) and their normal littermates (N/N). Mice were obtained from Dr BJ Scholte (Erasmus Medical Center, Cell Biology Department, Rotterdam, the Netherlands). Each animal genotype was checked at 21 days of age as previously described (Legssyer *et al.* 2006) using Taqman quantitative PCR multiplex analysis (Taqman, ABI PRISM 7700 Sequence Detection System, Applied Biosystems, Foster, CA, USA) of tail clip DNA. Experiments were carried out on 5-month-old male mice.

All adult animals had free access to drinking water and were fed *ad libitum* on a standard diet. To minimize bowel obstruction and to optimize long-term viability, a commercially available osmotic laxative containing polyethylene glycol (PEG-3350) and electrolytes (Movicol®) was continuously supplied at 6% in the drinking water (Cottart *et al.* 2007).

We also performed experiments on newborn homozygous mice for both mutations (S489X and F508del) and their control littermates at 1 day postnatal. The genotype of each individual animal was established by PCR amplification of genomic DNA isolated from tails (van Doorninck *et al.* 1995; Kent *et al.* 1997).

Examination of tracheal morphology

Newborn and adult CF mice from both models and littermate controls were anaesthetized with an intraperitoneal injection of ketamine ($80\,mg\,kg^{-1}$) (Virbac, France) and xylazine ($20\,mg\,kg^{-1}$) (Rompun, Bayer, Leverkusen, Germany). After exsanguination, the chest wall was opened and the trachea exposed. Measurements of the tracheal length from the cricoid cartilage to the carina and the outer diameter of each cartilage ring were determined using a stereomicroscope (Wild M5A, Switzerland). Normal and pathological tracheal cartilage rings were defined according to Pole *et al.* (2001). A 'normal' cartilage ring is defined as a single, continuous, 'C'-shaped cartilage ring, or a ring with a minor peripheral bifurcation or with a peripheral or midline bridge to an adjacent tracheal cartilage ring, in the absence of any other abnormality. A pathological tracheal cartilage ring is defined as an interrupted, fused, incomplete ring or a ring with a disrupted peripheral bifurcation.

Tracheal malformation was assessed by direct microscopic observation backed up by high magnification photographs and subsequent histological analyses. Two different histological procedures were used: (1) the larynx, trachea and lungs were excised as a single block and placed in 70% ethanol for a week, then stained in a mixture of 95% ethanol, glacial acetic acid and 1% Alcian blue (pH 2.5) at the ratio of 8 : 2 : 1 for 24 h (Pole *et al.* 2001); (2) the entire or partial trachea was excised and immersed in 10% formalin for 5 days. All tissue samples were paraffin-embedded and transversally or longitudinally cut into 4 μm sections. Tissue sections were stained with Masson's trichrome or Alcian blue (1% in H_2SO_4 10%) and examined under light microscopy by an experienced pathologist blinded to the mice genotype.

Contraction measurement on isolated tracheal rings

Mice (*Cftr*$^{+/+}$ and *Cftr*$^{-/-}$) were anaesthetized with a ketamine–xylazine solution and killed by cervical dislocation according to the animal care and local ethics committee. The mouse trachea was removed and placed into Krebs solution containing (mM): 120 NaCl, 4.7 KCl, 2.5 $CaCl_2$, 1.2 $MgCl_2$, 1.2 KH_2PO_4, 15 $NaHCO_3$, 11.1 D-glucose, pH 7.4. After separation of connective tissues, the mouse trachea was cut into two segments of the same length (a distal and a proximal part). Tracheas were mounted between a fixed clamp at the base of a water-jacketed 5 ml organ bath containing an oxygenated (95% O_2 and 5% CO_2) Krebs solution and an IT1–25 isometric force transducer (Emka Technologies, Paris, France) (Vandebrouck *et al.* 2006). All experiments were performed at a temperature of 37°C. A basal tension of 1 g was applied in all experiments. During 1 h, tissues were rinsed three times in Krebs solution and the basal tone was constantly monitored and adjusted to 1 g.

Cumulative concentration–response relationships for the constriction effect of carbachol prepared as a 1 mM stock solution in distilled water were determined in each tracheal portion. The EC_{50} was calculated as the carbachol concentration inducing a half-maximal constriction.

Measurement of ventilatory parameters

Experiments were carried out on adult *Cftr*$^{-/-}$ and F508del-CFTR mice and their respective littermate controls. Ventilatory parameters were recorded in a whole-body plethysmograph using the barometric method (Bartlett & Tenney, 1970). Calibration was performed at the beginning of experiments by several injections of 50 μl of air into the chamber. The pressure signal, as a result of breathing, was detected by using a differential pressure transducer (Validyne DP103/12; Validyne, Northridge, CA, US) connected to the animal chamber (400 ml) and to a reference chamber of the same volume. The spirogram was recorded and stored on a computer using respiratory acquisition software (CIO-DAS 1602/16 interface and ELPHY software) for off-line analysis.

Animals were weighed and placed in the chamber preheated at a temperature of 28–30°C. A thermistal probe (BIO-BIT14) was then inserted rectally and secured in place at the extremity of the tail and on the wall chamber. A wide protective muff was placed around the mouse to calm it down rapidly. The ventilatory parameters and colonic and chamber temperature were recorded for 20 min, at 5 min intervals, while the mouse breathed room air. The CO_2 concentration in the chamber was constantly $< 0.5\%$. The following variables were measured and calculated by a computer-assisted method: tidal volume (V_T), breathing rate (f_R), inspiratory and expiratory times (T_I and T_E). For every 5 min recording, values were averaged for 50–100 contiguous breaths.

Analysis of results and statistics

All values are given as means ± standard deviation. Statistical group comparison of ventilatory and morphometric data was evaluated using the Student *t* test. A χ^2 analysis was performed to compare structural abnormalities between *Cftr*$^{-/-}$ and *Cftr*$^{+/+}$ mice within each male or female group, and comparison of contractile responses of tracheal rings to carbachol was assessed by two-way ANOVA and multiple comparisons analysis using the Bonferroni test. *P* values of less than 0.05 were considered statistically significant.

Results

Structural and functional analyses in adult Cftr$^{-/-}$ mice

Tracheal morphology. Morphological analysis of the trachea was performed on 10 male and 15 female *Cftr*$^{-/-}$ adult mice and on 15 male and 10 female *Cftr*$^{+/+}$ adult mice. We first compared the tracheal length relative to the body length and the number of tracheal rings between *Cftr*$^{-/-}$ and *Cftr*$^{+/+}$ mice in each male or female group. No significant difference in tracheal length and the number of tracheal rings was observed between genotypes, whatever the sex. However, examination of the tracheal rings revealed the presence of cartilaginous ring abnormalities in most adult *Cftr*$^{-/-}$ mice (23/25) while only a few *Cftr*$^{+/+}$ mice (6/25) presented such abnormalities ($P < 0.001$) (Table 1). Moreover, as reported below, only *Cftr*$^{-/-}$ mice showed abnormalities of at least two cartilaginous rings. There was no influence of sex on the proportion of cartilage

Table 1. Distribution of abnormal tracheal rings in adult knockout (*Cftr*$^{-/-}$) and F508del-CFTR (ΔF/ΔF) mice and their respective littermate controls (*Cftr*$^{+/+}$ and N/N)

	Cftr$^{-/-}$		*Cftr*$^{+/+}$		ΔF/ΔF		N/N	
	Frequency	%	Frequency	%	Frequency	%	Frequency	%
Number of mice with abnormal rings	23/25*	92.0	6/25	24.0	11/12*	91.7	3/14	21.4
1 ring	4	16.0	6	24.0	1	8.3	2	14.3
2 to 3 rings	9	36.0	0	0	4	33.3	1	7.1
4 to 5 rings	7	28.0	0	0	6	50.0	0	0
> 5 rings	3	12.0	0	0	0	0	0	0
Site of defect								
Proximal trachea	23	92.0	5	20.0	3	25.0	2	14.3
Middle trachea	8	32.0	1	4.0	4	33.3	1	7.1
Distal trachea	1	4.0	0	0	5	41.7	1	0

Incidence and percentage occurrence of tracheal abnormalities are given for each group according to their number and location in the trachea as follows: proximal region (cartilage ring 1 to 5), middle region (cartilage ring 6 to 9) and distal region (cartilage ring 10 to 14). *Significant differences between CF and non-CF mice; $P < 0.001$.

defects observed in male (9/10) and female (14/15) *Cftr*$^{-/-}$ mice.

On macroscopic examination (Fig. 1*A*), a narrowing of the proximal part of the trachea was observed in numerous *Cftr*$^{-/-}$ mice (14/25). To evaluate segmental tracheal constriction accurately, we compared the mean external diameter values obtained from the three proximal rings to the corresponding values obtained from the three distal rings. The results showed that the external diameter of cartilaginous rings was significantly smaller in the proximal trachea than in the distal trachea of *Cftr*$^{-/-}$ mice whereas in control mice this measurement was similar in both tracheal segments (Fig. 1*B*).

The upper tracheal constriction observed in *Cftr*$^{-/-}$ mice was generally associated with frontal cracks or disruption of the first three to six cartilaginous rings below the cricoid cartilage as shown on Fig. 2*A*. Other tracheal malformations, such as incomplete cartilaginous rings, rings with lateral interruptions, with two frontal disruptions or with a disrupted bifurcation, were frequently detected in *Cftr*$^{-/-}$ mice. The number of abnormal rings and the site of these defects are detailed

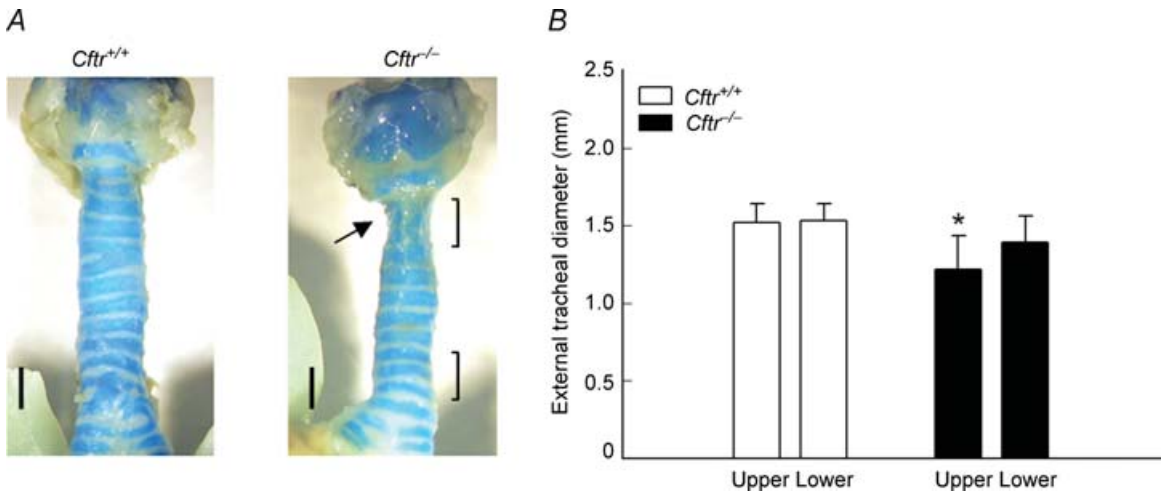

Figure 1. Morphology of the trachea of control (*Cftr*$^{+/+}$) and knockout (*Cftr*$^{-/-}$) adult mice showing abnormal cartilaginous rings and tracheal stenosis
A, frontal views of *Cftr*$^{+/+}$ and *Cftr*$^{-/-}$ tracheas from adult mice. Staining of the cartilage with Alcian blue underscores the narrowing of the upper trachea (arrow) in *Cftr*$^{-/-}$ mice (right). Scale bars, 2 mm. *B*, mean values (+ S.D.) of the external tracheal diameter of the upper compared to the lower trachea (indicated in square brackets in *A*, right panel) in male adult *Cftr*$^{+/+}$ ($n = 15$) and *Cftr*$^{-/-}$ ($n = 10$) mice. *Significant differences between the upper and lower portion of the trachea; $P < 0.05$ mice.

in Table 1. Abnormalities were more severe in the $Cftr^{-/-}$ mouse group as indicated by the finding that 76% of animals displayed two to seven abnormal cartilaginous rings while none of the control mice showed more than one abnormal ring. These tracheal malformations were predominantly located in the proximal portion of the trachea with 92% of the abnormalities within the first five cartilaginous rings (Table 1 and Fig. 2*B*).

Histological examination of longitudinal or transversal sections of tracheal rings confirmed the macroscopic observations (Fig. 3*A* and *B*). Indeed, in the areas of abnormal proximal trachea, normal connective tissue was present in the space that should have been filled up by cartilaginous rings. The microscopic analysis of the cartilaginous structure, either following Alcian blue or Masson's staining, did not show any major differences between tracheal rings from $Cftr^{-/-}$ and $Cftr^{+/+}$ mice, and no epithelial abnormalities and minor to no inflammation were detected in $Cftr^{-/-}$ mice (Fig. 3*C*).

Tracheal function. The contractile responses to carbachol of the proximal and distal portions of the trachea were assessed in $Cftr^{-/-}$ ($n = 6$) and $Cftr^{+/+}$ ($n = 6$) mice. The examination of tracheal structure revealed the presence of cartilaginous ring abnormalities in the proximal trachea of all six $Cftr^{-/-}$ mice while all $Cftr^{+/+}$ mice had normal architecture. As shown in Fig. 4, increasing concentrations of carbachol from 10^{-9} to 10^{-3} M produced a dose-dependent increase in contraction of both proximal and distal tracheal portions in both groups of mice. However, the proximal tracheal curve of $Cftr^{-/-}$ mice was clearly shifted to the right, indicating a decrease in the sensitivity of this tracheal segment to carbachol. The carbachol concentration inducing a half-maximal constriction (EC_{50}), was significantly higher in $Cftr^{-/-}$ mice as compared with $Cftr^{+/+}$ mice for the proximal part of the trachea ($EC_{50} = 698 \pm 15$ nM and 162 ± 23 nM, respectively) (Fig. 4*A* and *B*), but was similar for the distal part of the trachea ($EC_{50} = 239 \pm 18$ nM and 246 ± 21 nM, respectively) (Fig. 4*C* and *D*).

Ventilation. Ventilatory parameters were recorded during room air breathing in conscious $Cftr^{-/-}$ ($n = 6$) and $Cftr^{+/+}$ ($n = 6$) mice. As shown in Fig. 5, the mean tidal volume (± S.D.) was similar in both groups while the mean breathing rate (± S.D.) was significantly lower in $Cftr^{-/-}$ than in $Cftr^{+/+}$ mice, the difference resulting from a marked increase in both the inspiratory and expiratory times.

Taken together, this first set of morphometric and functional studies showed that $Cftr^{-/-}$ mice had severe cartilaginous ring defects, mainly located in the upper

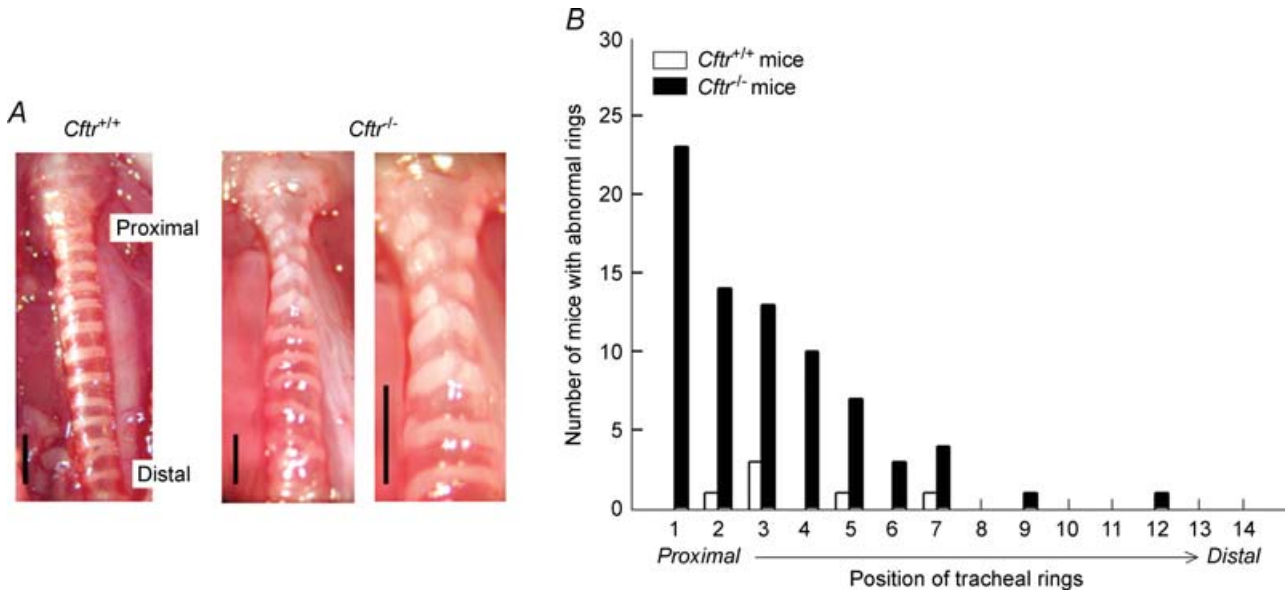

Figure 2. Morphology of the trachea of control ($Cftr^{+/+}$) and knockout ($Cftr^{-/-}$) adult mice showing abnormal cartilaginous rings and their localization in the trachea
A, frontal views of fresh unfixed tracheas from adult $Cftr^{+/+}$ and $Cftr^{-/-}$ mice. The upper trachea of $Cftr^{-/-}$ mice (right) shows cartilaginous rings with frontal disruptions. Scale bars, 2 mm. *B*, number of $Cftr^{+/+}$ mice (total group, $n = 25$) and $Cftr^{-/-}$ mice (total group, $n = 25$) showing cartilaginous defects from the proximal (ring no. 1) up to the distal (ring no. 14) trachea.

portion of the trachea, associated with a decreased sensitivity of proximal tracheal rings to carbachol and a decrease in the breathing rate.

Tracheal morphology and ventilation in adult F508del-CFTR mice

Morphological analyses of the trachea of 12 F508del-CFTR (ΔF/ΔF) and 14 control (N/N) mice showed that cartilaginous ring abnormalities were also present in 11 out of 12 ΔF/ΔF mice and that the tracheal ring defects had features similar to those described for *Cftr*$^{-/-}$ mice (Fig. 6*A*). These tracheal abnormalities, including one to four interrupted or segmented cartilaginous rings, were observed all along the trachea although more often located in the distal portion of the trachea (Table 1 and Fig. 6*B*).

Ventilation was recorded during room air breathing in seven conscious adult F508del-CFTR (ΔF/ΔF) and seven control (N/N) mice. As shown in Fig. 7, the mean tidal volume was significantly lower in ΔF/ΔF mice as compared with N/N mice. Although the mean breathing rate was similar in both groups, the expiratory time was significantly longer in ΔF/ΔF mice while the inspiratory time did not differ between both groups.

Tracheal morphology in newborn Cftr$^{-/-}$ and F508del-CFTR mice

Twenty-three newborn mice from six different litters at 1 day postnatal were genotyped and categorized into normal homozygous (*Cftr*$^{+/+}$; $n = 8$) and knockout (*Cftr*$^{-/-}$; $n = 15$) mice. Examination of the trachea

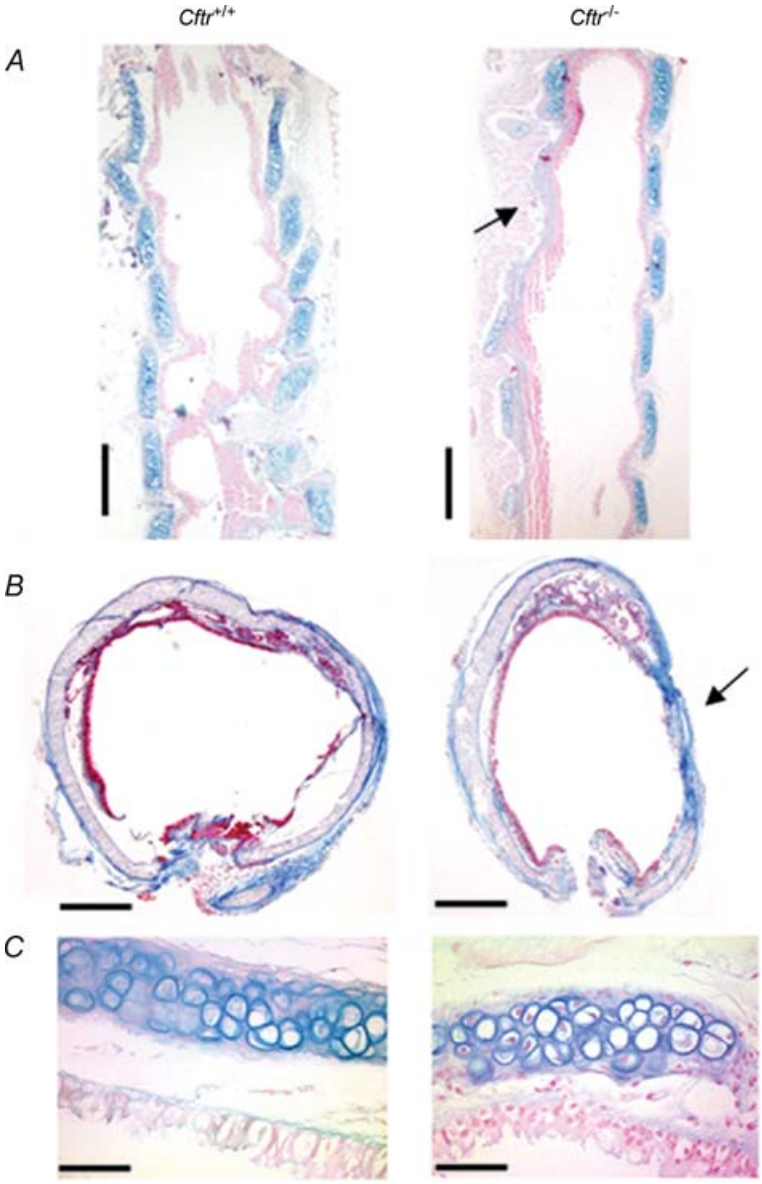

Figure 3. Histology of tracheal cartilaginous rings from adult *Cftr*$^{+/+}$ and *Cftr*$^{-/-}$ mice
A and *B*, longitudinal (*A*) and transverse (*B*) tracheal sections of cartilaginous rings of the upper trachea from adult *Cftr*$^{+/+}$ (left) and *Cftr*$^{-/-}$ (right) mice. Scale bars, 1 mm in *A*, and 2 mm in *B*. Note the presence of connective tissue instead of cartilage (arrow) in *Cftr*$^{-/-}$ mice. *C*, high magnifications of tracheal ring cartilage after Alcian blue staining of trachea of *Cftr*$^{+/+}$ (left) and *Cftr*$^{-/-}$ (right) mice showing the absence of abnormalities in the cartilage and only minor to no mucosal inflammation in *Cftr*$^{-/-}$ mice. Scale bars, 50 μm.

revealed that 13 out of 15 newborn *Cftr*$^{-/-}$ mice had at least one cartilaginous ring defect and 5 out of 15 displayed severe abnormalities with the presence of two to six ring defects (Table 2). One or two frontal interruptions, incomplete rings or rings with a disrupted bifurcation (Fig. 8*A*) characterized abnormal cartilaginous rings. Such tracheal abnormalities were mainly localized to the proximal portion of the trachea, although no significant tracheal stenosis could be detected (Table 2). The *Cftr*$^{+/+}$ newborn mice showed no tracheal malformation.

Histological examination of tracheal longitudinal sections showed a general disorganization of the trachea cartilaginous structure of newborn *Cftr* knockout mice as compared to their normal homozygous littermates.

Tracheal abnormalities were also observed in newborn F508del-CFTR mice where 4 out of 5 animals had between two and six cartilaginous ring defects (Table 2 and Fig. 8*B*). This was comparable to that described in newborn *Cftr*$^{-/-}$ mice although there was no specific localization of the defects on the trachea. No tracheal malformations were detected in littermate control mice.

Discussion

The present study demonstrates for the first time that adult *Cftr*$^{-/-}$ mice exhibit structural abnormalities of the extrathoracic airways, characterized by disrupted or

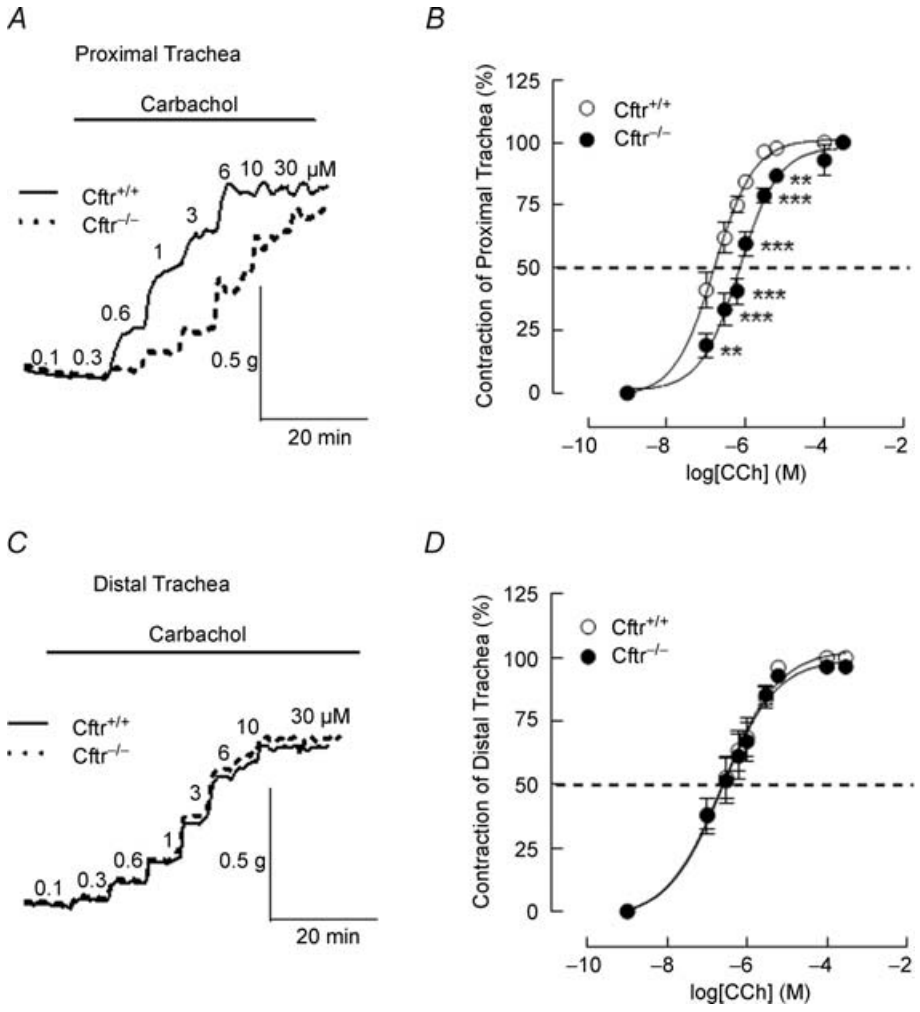

Figure 4. Contractile response to carbachol of isolated tracheal segments in adult *Cftr*$^{+/+}$ and *Cftr*$^{-/-}$ mice

A and *C*, typical traces from experiments performed with proximal (*A*) and distal (*C*) portions of trachea in response to increasing concentrations of carbachol in a *Cftr*$^{+/+}$ (continuous line) and a *Cftr*$^{-/-}$ (dotted line) mouse. *B* and *D*, mean values (± SEM) of the constricting effect of carbachol on the proximal (*B*) and distal (*D*) portions of trachea expressed in per cent from maximal contraction in *Cftr*$^{+/+}$ (○, $n = 6$) and *Cftr*$^{-/-}$ (●, $n = 6$) mice. Dotted lines represent the carbachol concentration (EC_{50}) inducing a half-maximal constriction. Significant differences at several contraction levels between *Cftr*$^{-/-}$ and *Cftr*$^{+/+}$ mice are given: $^{**}P < 0.01$, $^{***}P < 0.001$.

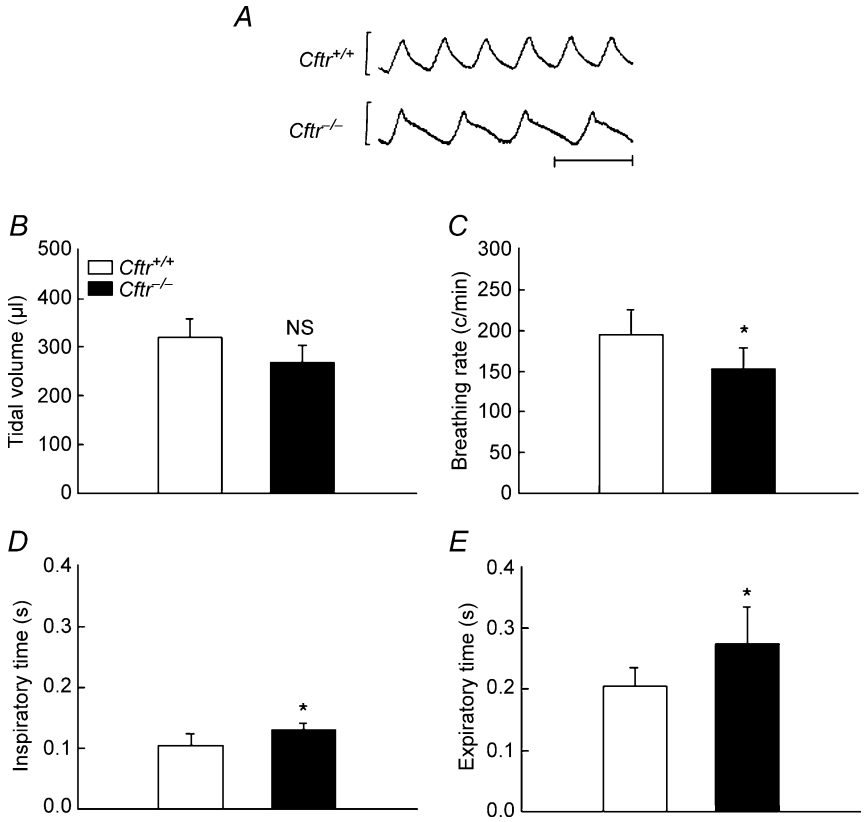

Figure 5. Ventilation of conscious adult control (*Cftr*$^{+/+}$) and knockout (*Cftr*$^{-/-}$) mice while breathing room air
A, typical spirograms of a *Cftr*$^{+/+}$ mice and a *Cftr*$^{-/-}$ mice. The scale bar for the tidal volume corresponds to 300 μl. The scale bar for time corresponds to 0.5 s. *B–E*, average values (+ S.D.) of ventilatory variables in *Cftr*$^{+/+}$ (□, $n = 6$) and *Cftr*$^{-/-}$ (■, $n = 6$) mice: tidal volume (*B*), breathing rate (*C*), inspiratory time (*D*) and expiratory time (*E*). *Significant differences between *Cftr*$^{+/+}$ and *Cftr*$^{-/-}$ mice; $P < 0.05$.

incomplete cartilage rings. If several cartilage rings of the upper trachea are frontally interrupted, extensive tracheal stenosis ensues. This may contribute to tracheal dysfunction and an abnormal breathing pattern.

The high rate of tracheal abnormalities in adult *Cftr*$^{-/-}$ mice homozygous for the S489X mutation of the CFTR protein, in contrast to that observed in control *Cftr*$^{+/+}$ mice, suggests that these abnormalities could be directly

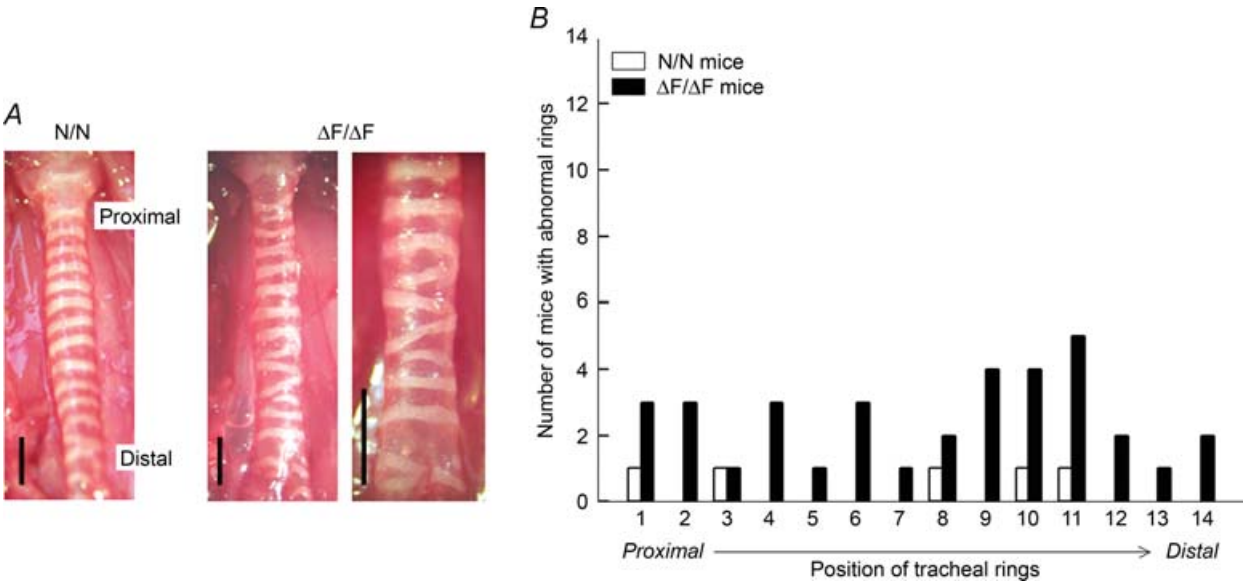

Figure 6. Morphology of the trachea of control (N/N) and F508del-CFTR (ΔF/ΔF) adult mice showing abnormal cartilaginous rings and their localization in the trachea
A, frontal views of fresh unfixed tracheas from adult N/N and ΔF/ΔF mice showing interrupted or segmented cartilaginous rings in the trachea of ΔF/ΔF mice (right). Scale bars, 2 mm. *B*, number of N/N mice (total group, $n = 14$) and ΔF/ΔF mice (total group, $n = 12$) showing cartilaginous defects from the proximal (ring no. 1) up to the distal (ring no. 14) trachea.

Table 2. Distribution of abnormal tracheal rings in newborn knockout (*Cftr*$^{-/-}$) and F508del-CFTR (ΔF/ΔF) mice and their respective controls (*Cftr*$^{+/+}$ and N/N)

	Cftr$^{-/-}$		*Cftr*$^{+/+}$	ΔF/ΔF		N/N
	Frequency	%	Frequency	Frequency	%	Frequency
Number of mice with abnormal rings	13/15*	86.7	0/8	5/5*	100	0/5
1 ring	5	33.3	0	1/5	20	0
2–6 rings	8	53.3	0	4/5	80	0
Site of defect						
Proximal trachea	10	66.7	0	2/5	40	0
Middle trachea	3	20.0	0	4/5	80	0
Distal trachea	1	6.7	0	2/5	40	0

Incidence and percentage occurrence of tracheal abnormalities are given for each group of CFTR-deficient mice according to their number and site of defect in the trachea. *Significant differences between CF and non-CF mice; $P < 0.001$.

related to the Cftr mutation. To test this hypothesis further, we studied a group of mice with the most common mutation (F508del) and their littermate controls. Our findings show that the trachea of adult F508del-CFTR mice also exhibit cartilage ring abnormalities, which strongly implicates the *Cftr* gene in these tracheal anomalies. However, in contrast to that observed in *Cftr*$^{-/-}$ mice, the cartilage defects detected in F508del-CFTR mice were

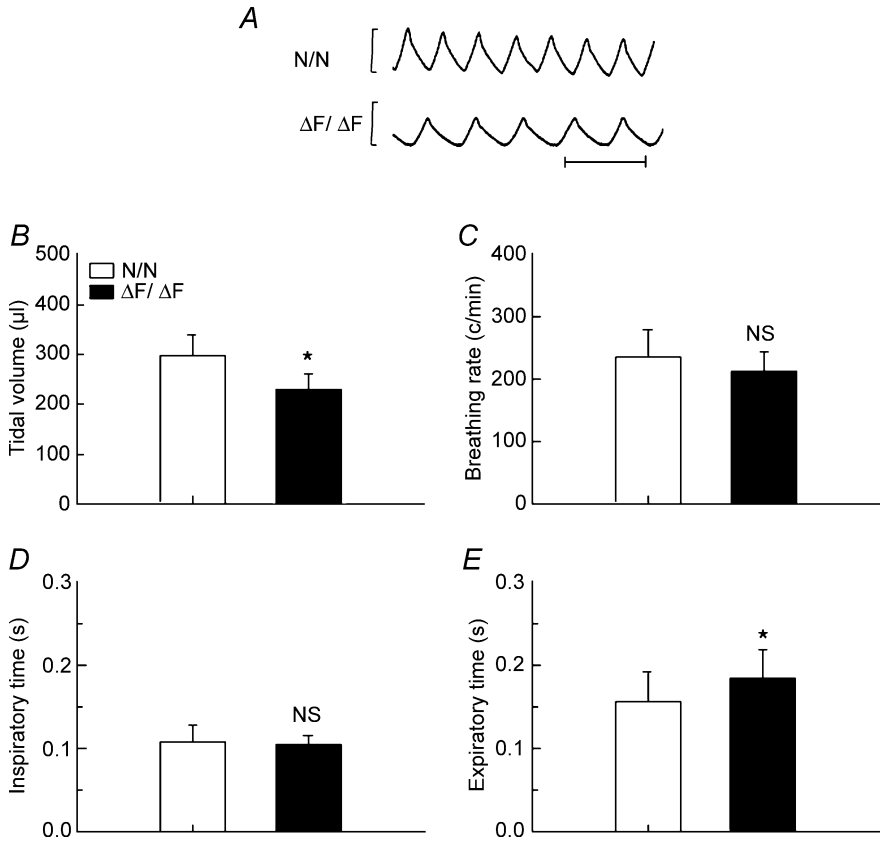

Figure 7. Ventilation of conscious adult control (N/N) and F508del-CFTR (ΔF/ΔF) mice while breathing room air

A, typical spirograms of an N/N mice and a ΔF/ΔF mice. The scale bar for the tidal volume corresponds to 300 μl. The scale bar for time corresponds to 0.5 s. *B–E*, average values (+ S.D.) of ventilatory variables in N/N (□, $n = 7$) and ΔF/ΔF (■, $n = 7$) mice: tidal volume (*B*), breathing rate (*C*), inspiratory time (*D*) and expiratory time (*E*). *Significant differences between N/N and ΔF/ΔF mice; $P < 0.05$.

present all along the trachea, with only a slight predominance in the distal portion. Although these two CF mouse models have a mutated *Cftr* gene, they are genetically different. *Cftr*$^{-/-}$ mice harbour a mutation coding for a CFTR mRNA defective in exon 10 that leads to a truncated non-functional protein (Xu *et al.* 1998), whereas F508del-CFTR mice have a low but detectable residual CFTR activity (van Doorninck *et al.* 1995). Moreover, the two CF mouse models have been developed in different genetic backgrounds that are known to influence the development of different lung phenotypes (Kent *et al.* 1997; Innes & Dorin, 2001; Haston *et al.* 2002). In human studies, recent findings clearly show that secondary genetic factors, besides CFTR, play an important role in determining the severity of CF lung disease (Boyle, 2007). In this context, one can speculate that the different genetic backgrounds of the two CF mice models may act upon the CF tracheal phenotype through potential modifier loci that affect the expression of specific genes involved in cartilage ring formation. Therefore, differences in the location of tracheal abnormalities reported in the present study may also depend on either the genetic mutation and/or the mouse strain genetic background.

The underlying mechanisms of such tracheal abnormalities could involve postnatal inflammatory processes related to the cystic fibrosis disease. However, only minor inflammation was detected and it is unlikely that such a mechanism will lead to the structural changes observed. Moreover, we found similar anomalies in newborn *Cftr*$^{-/-}$ and F508del-CFTR mice, thereby suggesting that these cartilaginous ring defects represent congenital malformations. Therefore, the important question arising from these observations concerns the molecular mechanisms governing tracheal development in relation to CFTR protein dysfunction.

Reciprocal interactions between epithelial cells derived from the foregut endoderm and the surrounding mesenchyme leading to cartilage ring formation are known to govern tracheal morphogenesis. Various gene products play an important role in such cartilage genesis. Among them, TRAF4, a member of the tumour necrosis factor receptor-associated factor (TRAF) family, deserves special attention as similar tracheal abnormalities to those we observed in CF mice have been reported in two recent studies describing TRAF4-deficient mice (Shiels *et al.* 2000; Regnier *et al.* 2002). Both studies showed that a TRAF4 deficiency leads to tracheal malformation with cartilaginous ring disruption and upper tracheal constriction. Moreover, Shiels *et al.* (2000) reported reduced respiratory airflow resulting from tracheal stenosis, which is consistent with the altered breathing rate that we observed in our *Cftr*$^{-/-}$ mice. Therefore, the similarities between their results and the tracheal defects detected in the present study led us to consider that alteration to the upper airways during lung development in CFTR-deficient mice may be associated with a deregulation in TRAF4 expression. Moreover, TRAF4 expression was detected in the enamel epithelium during murine tooth development (Ohazama *et al.* 2003) and abnormal enamel formation has been observed in the teeth of *Cftr*$^{-/-}$ mice (Snouwaert *et al.* 1992; Wright *et al.* 1996). In the present study, we also noted that the *Cftr*$^{-/-}$ and F508del-CFTR mice exhibited chalky, white incisors as

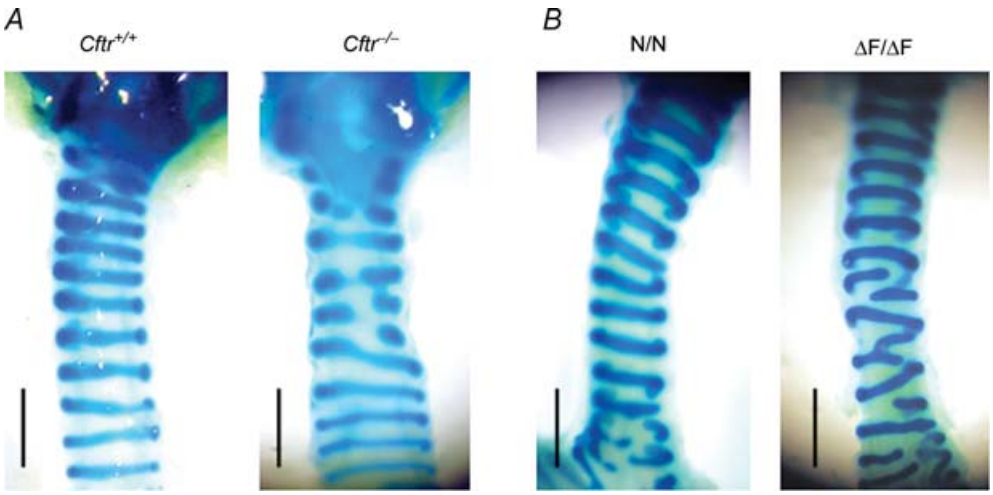

Figure 8. Morphology of the trachea of newborn CF mice of both CF mice models (*Cftr*$^{-/-}$ and ΔF/ΔF) and their respective controls (*Cftr*$^{+/+}$ and N/N) showing abnormal cartilaginous rings
A, frontal views of fresh tracheas from newborn *Cftr*$^{+/+}$ and *Cftr*$^{-/-}$ mice (*A*), and from newborn control (N/N) and F508del-CFTR (ΔF/ΔF) mice (*B*). Staining of the cartilage with Alcian blue reveals tracheal ring disruptions localized to the proximal trachea of *Cftr*$^{-/-}$ mice and to the distal trachea of (ΔF/ΔF) mice. Scale bars, 1 mm in *A* and *B*.

compared with the hard, yellow-brown enamel of normal mice (data not shown). Interestingly, these two models of CF mice exhibit tracheal abnormalities as described in the present study. Several other genes might be involved in tracheal ring malformation. Sonic hedgehog (Shh) is expressed in the epithelial cell lining of the conducting airways and is required for the specification of the site and extent of tracheo-bronchial cartilage (Miller *et al.* 2004), while Sox9 is expressed in the developing upper respiratory tract from E9 to E16 and is involved in chondrocyte differentiation in cartilaginous rings (Elluru & Whitsett, 2004).

Other direct or indirect mechanisms that are related to an abnormal CFTR activity may influence the development of cartilage rings. Indeed, abnormal CFTR expression and the resultant dysfunction of this chloride channel in developing tracheal tissues could disrupt their formation through an abnormal ion concentration in the extracellular matrix. In this way, the local growth of cartilage is known to depend on surrounding tissues (Mankarious *et al.* 2006) and an altered tracheal epithelium related to dysfunction of CFTR expression may compromise its normal development. In addition, CFTR is highly expressed in the submucosal glands which are abnormally distributed in the proximal trachea of CF mice (Borthwick *et al.* 1999) and SMG hyperplasia may affect local growth factors (Mankarious *et al.* 2006). However, the histological examination of the upper airway of our $Cftr^{-/-}$ mice did not reveal any striking pathological changes that support these hypotheses such as gland duct dilatation in the proximal trachea and destructive changes in the epithelia of upper airways, as firstly described (Snouwaert *et al.* 1992).

The severe alteration in the tracheal architecture that we observed in CFTR-deficient mice leads us to question its deleterious effects on the mechanical properties of the trachea and on respiratory function. In the present study we explored the tracheal function by analysing the contractile response to carbachol of tracheal segments from $Cftr^{-/-}$ and $Cftr^{+/+}$ mice. Our results show that the proximal portion of the trachea of $Cftr^{-/-}$ mice was less sensitive to carbachol implying a marked loss in the contractile capacity of the trachea. This functional deficit can be related to the presence of numerous disrupted cartilage rings of the proximal trachea. Yet, the cartilaginous structure of the trachea provides support for the airway wall and is an elastic wall that resists airway narrowing. Therefore, such cartilage defects probably weaken the tracheal support and contribute to the altered airway mechanical function. However, this result can also be explained by altered smooth muscle activity related to a deficiency in CFTR expression as recently shown in smooth muscle cells (Vandebrouck *et al.* 2006). Indeed, two studies showed impaired relaxation of a precontracted tracheal segment in $Cftr^{-/-}$ mice (Mhanna *et al.* 2001; Vandebrouck *et al.* 2006). In addition, reduction of the neural network innervating airway smooth muscle and the smooth muscle mass observed in the developing airway of $Cftr^{-/-}$ mice might contribute to alterations in tracheal function (Pan *et al.* 2006).

Loss of tracheal cartilage may predispose to collapse of the airways and, hence, limit airflow. We previously demonstrated that juvenile and adult $Cftr^{-/-}$ mice had a lower minute ventilation than $Cftr^{+/+}$ mice (Bonora *et al.* 2004; Cottart *et al.* 2007). In the present study, our results show that the breathing rate, a component of the breathing pattern, is significantly lower in $Cftr^{-/-}$ mice resulting from an increased duration of the inspiratory and expiratory phases, with the presence of expiratory braking. In F508del-CFTR mice, the expiratory duration is slightly decreased as compared with control mice while no significant difference is observed in the inspiratory duration. These changes in the breathing pattern may reflect airway obstruction or a bronchial diameter modification induced by reduced compliance (Cohen *et al.* 2004). However, these two features of the altered lung function are not clearly established in CF mice. Nevertheless, the lengthening of respiratory cycles observed in $Cftr^{-/-}$ mice, and to a lesser extent in F508del-CFTR mice, may originate from mechanical alterations in the extrathoracic airway (Sanchis *et al.* 1990). Indeed, upper airways, in particular the larynx, are known to play a major role in respiratory activity (Bartlett, 1989), and a dysfunction of the sublaryngeal area due to cartilage defects may have deleterious consequences on the breathing pattern.

Interestingly, the upper tracheal constriction observed in adult $Cftr^{-/-}$ mice was absent or not as marked in newborn mice. Since newborns are known to have extremely compliant tracheal cartilage (Penn *et al.* 1989), the presence of congenitally malformed rings, as described in the present study, may overlap with the maturational process of cartilage stiffness and promote tracheal stenosis.

In CF patients, post mortem analyses of tracheas from young adults were found to be abnormally flaccid with the outlines of the tracheal rings irregular and partly resorbed (Griscom *et al.* 1987). These pathological abnormalities were thought to originate from vigorous coughing, mechanical ventilation or chronic inflammation. However, based upon the present results, it could be suggested that prior to these postnatal events, abnormal cartilaginous rings may already be present at birth due to altered tracheal development related to CFTR dysfunction. Indeed, the pathogenesis of lung disease in CF, particularly in early life, has not been fully characterized. It is likely that an alteration in the dynamics of the respiratory system may contribute to the sequence of events leading to the onset of pulmonary infection and inflammation.

To conclude, the present study demonstrates tracheal abnormalities in CFTR-deficient mice. The marked cartilaginous defects observed for $Cftr^{-/-}$ mice were associated with subsequent tracheal stenosis and deficient tracheal function that may therefore be part of an altered respiratory airflow. Moreover, the presence of such abnormal cartilage rings in newborn animals suggests that the tracheal phenotype of CF mice occurred during development and that an abnormal *Cftr* gene may alter expression of several other genes involved in tracheal ring formation. Our present findings prompt us to investigate further the mechanisms underlying the occurrence of tracheal abnormalities during development in CFTR-deficient mice, and to study the tracheal structure, using non-invasive methods, in young CF patients.

References

Bartlett D Jr (1989). Respiratory functions of the larynx. *Physiol Rev* **69**, 33–57.

Bartlett D Jr & Tenney SM (1970). Control of breathing in experimental anemia. *Respir Physiol* **10**, 384–395.

Bonora M, Bernaudin JF, Guernier C & Brahimi-Horn MC (2004). Ventilatory responses to hypercapnia and hypoxia in conscious cystic fibrosis knockout mice Cftr. *Pediatr Res* **55**, 738–746.

Borthwick DW, West JD, Keighren MA, Flockhart JH, Innes BA & Dorin JR (1999). Murine submucosal glands are clonally derived and show a cystic fibrosis gene-dependent distribution pattern. *Am J Respir Cell Mol Biol* **20**, 1181–1189.

Boyle MP (2007). Strategies for identifying modifier genes in cystic fibrosis. *Proc Am Thorac Soc* **4**, 52–57.

Bureau MA, Lupien L & Begin R (1981). Neural drive and ventilatory strategy of breathing in normal children, and in patients with cystic fibrosis and asthma. *Pediatrics* **68**, 187–194.

Cheng SH, Gregory RJ, Marshall J, Paul S, Souza DW, White GA, O'Riordan CR & Smith AE (1990). Defective intracellular transport and processing of CFTR is the molecular basis of most cystic fibrosis. *Cell* **63**, 827–834.

Coates AL, Desmond KJ, Milic-Emili J & Beaudry PH (1981). Ventilation, respiratory center output, and contribution of the rib cage and abdominal components to ventilation during CO_2 rebreathing in children with cystic fibrosis. *Am Rev Respir Dis* **124**, 526–530.

Cohen JC, Lundblad LK, Bates JH, Levitzky M & Larson JE (2004). The 'Goldilocks effect' in cystic fibrosis: identification of a lung phenotype in the cftr knockout and heterozygous mouse. *BMC Genet* **5**, 21.

Cottart CH, Bonvin E, Rey C, Wendum D, Bernaudin JF, Dumont S, Lasnier E, Debray D, Clement A, Housset C & Bonora M (2007). Impact of nutrition on phenotype in CFTR-deficient mice. *Pediatr Res* **62**, 528–532.

Durie PR, Kent G, Phillips MJ & Ackerley CA (2004). Characteristic multiorgan pathology of cystic fibrosis in a long-living cystic fibrosis transmembrane regulator knockout murine model. *Am J Pathol* **164**, 1481–1493.

Elluru RG & Whitsett JA (2004). Potential role of Sox9 in patterning tracheal cartilage ring formation in an embryonic mouse model. *Arch Otolaryngol Head Neck Surg* **130**, 732–736.

Engelhardt JF, Yankaskas JR, Ernst SA, Yang Y, Marino CR, Boucher RC, Cohn JA & Wilson JM (1992). Submucosal glands are the predominant site of CFTR expression in the human bronchus. *Nat Genet* **2**, 240–248.

Griscom NT, Vawter GF & Stigol LC (1987). Radiologic and pathologic abnormalities of the trachea in older patients with cystic fibrosis. *AJR Am J Roentgenol* **148**, 691–693.

Haston CK, Corey M & Tsui LC (2002). Mapping of genetic factors influencing the weight of cystic fibrosis knockout mice. *Mamm Genome* **13**, 614–618.

Ianowski JP, Choi JY, Wine JJ & Hanrahan JW (2007). Mucus secretion by single tracheal submucosal glands from normal and cystic fibrosis transmembrane conductance regulator knockout mice. *J Physiol* **580**, 301–314.

Innes BA & Dorin JR (2001). Submucosal gland distribution in the mouse has a genetic determination localized on chromosome 9. *Mamm Genome* **12**, 124–128.

Kent G, Iles R, Bear CE, Huan LJ, Griesenbach U, McKerlie C, Frndova H, Ackerley C, Gosselin D, Radzioch D, O'Brodovich H, Tsui LC, Buchwald M & Tanswell AK (1997). Lung disease in mice with cystic fibrosis. *J Clin Invest* **100**, 3060–3069.

Kent G, Oliver M, Foskett JK, Frndova H, Durie P, Forstner J, Forstner GG, Riordan JR, Percy D & Buchwald M (1996). Phenotypic abnormalities in long-term surviving cystic fibrosis mice. *Pediatr Res* **40**, 233–241.

Legssyer R, Huaux F, Lebacq J, Delos M, Marbaix E, Lebecque P, Lison D, Scholte BJ, Wallemacq P & Leal T (2006). Azithromycin reduces spontaneous and induced inflammation in ΔF508 cystic fibrosis mice. *Respir Res* **7**, 134.

Mankarious LA, Pires VL & Rudnick JA (2006). Local control of murine subglottis development. *Otolaryngol Head Neck Surg* **134**, 843–847.

Mhanna MJ, Ferkol T, Martin RJ, Dreshaj IA, van Heeckeren AM, Kelley TJ & Haxhiu MA (2001). Nitric oxide deficiency contributes to impairment of airway relaxation in cystic fibrosis mice. *Am J Respir Cell Mol Biol* **24**, 621–626.

Miller LA, Wert SE, Clark JC, Xu Y, Perl AK & Whitsett JA (2004). Role of Sonic hedgehog in patterning of tracheal-bronchial cartilage and the peripheral lung. *Dev Dyn* **231**, 57–71.

Ohazama A, Courtney JM & Sharpe PT (2003). Expression of TNF-receptor-associated factor genes in murine tooth development. *Gene Expr Patterns* **3**, 127–129.

Pan J, Luk C, Kent G, Cutz E & Yeger H (2006). Pulmonary neuroendocrine cells, airway innervation, and smooth muscle are altered in Cftr null mice. *Am J Respir Cell Mol Biol* **35**, 320–326.

Penn RB, Wolfson MR & Shaffer TH (1989). Developmental differences in tracheal cartilage mechanics. *Pediatr Res* **26**, 429–433.

Pole RJ, Qi BQ & Beasley SW (2001). Abnormalities of the tracheal cartilage in the rat fetus with tracheo-oesophageal fistula or tracheal agenesis. *Pediatr Surg Int* **17**, 25–28.

Regnier CH, Masson R, Kedinger V, Textoris J, Stoll I, Chenard MP, Dierich A, Tomasetto C & Rio MC (2002). Impaired neural tube closure, axial skeleton malformations, and tracheal ring disruption in TRAF4-deficient mice. *Proc Natl Acad Sci U S A* **99**, 5585–5590.

Sanchis J, Diez-Betoret JL, Casan P & Milic-Emili J (1990). The pattern of resting breathing in patients with upper airway obstruction. *Eur Respir J* **3**, 521–526.

Shiels H, Li X, Schumacker PT, Maltepe E, Padrid PA, Sperling A, Thompson CB & Lindsten T (2000). TRAF4 deficiency leads to tracheal malformation with resulting alterations in air flow to the lungs. *Am J Pathol* **157**, 679–688.

Snouwaert JN, Brigman KK, Latour AM, Malouf NN, Boucher RC, Smithies O & Koller BH (1992). An animal model for cystic fibrosis made by gene targeting. *Science* **257**, 1083–1088.

Vandebrouck C, Melin P, Norez C, Robert R, Guibert C, Mettey Y & Becq F (2006). Evidence that CFTR is expressed in rat tracheal smooth muscle cells and contributes to bronchodilation. *Respir Res* **7**, 113.

van Doorninck JH, French PJ, Verbeek E, Peters RH, Morreau H, Bijman J & Scholte BJ (1995). A mouse model for the cystic fibrosis ΔF508 mutation. *EMBO J* **14**, 4403–4411.

Welsh MJ, Ramsey BW, Accurso F & Cutting GR (2001). *The Metabolic and Molecular Basis of Inherited Disease*, Vol. III, Part 21, ed. Scriver CR, Beaudet AL, Sly WS, Valle D, Childs B & Vogelstein, B. 5121–5188. McGraw-Hill Inc., New York.

Wright JT, Kiefer CL, Hall KI & Grubb BR (1996). Abnormal enamel development in a cystic fibrosis transgenic mouse model. *J Dent Res* **75**, 966–973.

Xu Z, Gupta V, Lei D, Holmes A, Carlson E & Gruenert DC (1998). In-frame elimination of exon 10 in Cftrtm1Unc CF mice. *Gene* **211**, 117–123.

Acknowledgements

We thank members of the CNRS CDTA (Centre de Développement des Techniques Avancées pour l'Expérimentation Animale, Orléans, France) for providing us with the *Cftr*^{tm1Unc} mice and Dr BJ Scholte (Erasmus Medical Centre, Rotterdam, the Netherlands) for providing us with the *Cftr*^{tm1Eur} F508del mice. We also thank Isabelle Renaud who took care of the animals at the St-Antoine facilities, Lydie Germain, Nicole Maurin and Anne-Marie Vojtek for their help in histological analysis and Olivier Tabary for his expertise with the images. This study was supported by grants from INSERM, Assistance Publique Hôpitaux de Paris, Université Pierre et Marie Curie and EuroCareCF (EU FP6 LSHM-CT-2005-018923).